

A multichannel neutron flux monitoring system for a boron neutron capture therapy facility.

**T.A. Bykov,^{a,b} D.A. Kasatov,^{a,b} A.M. Koshkarev,^{a,b} A.N. Makarov,^{a,b} V.V. Porosev,^{a,b,1}
G.A. Savinov,^a I.M. Shchudlo,^{a,b} S.Yu. Taskaev^{a,b}**

^a*Budker Institute of Nuclear Physics,
Lavrentiev ave. 11, Novosibirsk 630090, RUSSIA*

^b*Novosibirsk State University,
Pirogova st. 2, Novosibirsk 630090, RUSSIA*

E-mail: porosev@inp.nsk.su

ABSTRACT: The progress in the design of new accelerator-based neutron sources for boron neutron capture therapy (BNCT) generated new requirements to the detector systems to monitor the particle flux during the irradiation of patients. In the current research, we evaluated basic parameters of a twin scintillator-over-fiber system with a silicon photo-multiplier readout based on boron-enriched and boron-free plastic scintillators. The presented results showed that the proposed system could be used for monitoring of neutron flux, and the designed detector system demonstrated good linearity, up to $\sim 2\text{mA}$, limited by accelerator specifications at that time.

KEYWORDS: Plastic scintillator, neutron detector, silicon photomultipliers

¹Corresponding author.

Contents

1	Introduction.	2
2	Scintillators and optical fibers.	2
3	Sensor set-up.	3
4	Initial trials.	6
5	Dual threshold approach.	7
6	Results and discussion.	8
7	Conclusion.	9
8	Acknowledgments	10

1

2 **1 Introduction.**

3 The advent of a new generation of the accelerator-based epithermal neutron sources for BNCT
 4 raised the question of new diagnostic methods to control the contribution of neutrons to the total
 5 radiation dose of patients. The most common approach to solving this problem is using two detectors
 6 simultaneously: the first one, sensitive to gamma radiation, and the second one, sensitive to gamma
 7 radiation and neutrons. The difference in readings of these two detectors allows us to estimate the
 8 contribution of the neutron component more accurately [1]. Plastic scintillation detectors with an
 9 optical fiber readout are successfully used for gamma and high-energy electron dosimetry [2]. A
 10 similar approach for neutrons was developed in Japan [3, 4]. In this research, we tested the basic
 11 parameters of a scintillator-over-fiber detector with a silicon photomultiplier (SiPM) readout. The
 12 application of the SiPMs instead of vacuum photo-multipliers has several advantages. First, they
 13 are more compact, have excellent single photo-electron resolution and higher quantum efficiency,
 14 and are cheaper by far. Additionally, progress in the design of a related readout electronics made it
 15 possible to create multichannel readout systems based on dedicated ASICs. Further, we present our
 16 results on the creation of a dose monitoring system for a proton tandem accelerator with a lithium
 17 neutron producing target, proposed at BINP [5].

18 **2 Scintillators and optical fibers.**

19 Two types of polystyrene-based scintillators: SC-301, without boron, and SC-331, enriched with
 20 boron, which have a fast response of ~ 2.5 ns, are produced in Russia [6]. According to their
 21 specifications, both of them use the same fluorophores and SC-331 contains 0.9% natural isotope
 22 Boron-10. The maximum of the emission spectrum of the scintillator is situated near 425 nm.
 23 The light yield of SC-331 is 8600 photons/MeV, and for SC-301 it is approximately 25% higher.
 24 Polymer-based Optical Fibers (POFs) are widely used for data communications. One of the most
 25 popular materials used for their production is polymethylmethacrylate (PMMA). Polystyrene (PS)
 26 or polycarbonate-based fibers have a higher refraction index, but because of higher attenuation
 27 they are not generally used for data communications. Main parameters of the tested POFs with a
 28 diameter of 1 mm are presented in the Table 1.

Table 1. Main parameters of the tested POFs.

Name	Numerical aperture	Core material
ASAHI, SB-1000	0.60	PMMA
mitsubishi, CK-40	0.50	PMMA
KURARAY, CLEAR-PSMSJ	0.72	PS

29 Figure 1 demonstrates the light transmission as a function of the POF length, measured at a
 30 wavelength of 405 nm. The solid lines in the figure show the calculated fraction of transmitted
 31 light depending on the fiber length with a characteristic absorption length of 1.8 meter (curve 1)
 32 and 26.5 meter (curve 2). The measurements were done on a stand with a LED driver SP5601

1 (CAEN)¹ as a light source. Transmitted optical pulses were detected by MPPC S13360-3050CS
 2 (HAMAMATSU), followed by a home-made amplifier based on THS3202 (Texas Instruments)²
 3 with a gain of ~ 20 . Amplified signals were recorded with a desktop waveform digitizer DT5720
 4 (CAEN). All PMMA-based fibers exhibit similar behavior with transmission of $\sim 70\%$ signal at a
 5 distance of ~ 9 m, while the polystyrene-based fiber showed more significant signal degradation.

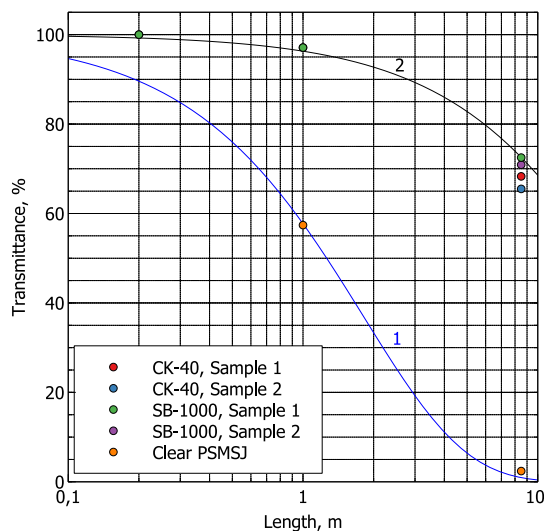


Figure 1. Light transmission of POFs under study.

6 3 Sensor set-up.

7 To estimate the fraction of optical photons detected at the distal end of a POF when the scintillator
 8 is irradiated by thermal neutrons, we performed Monte-Carlo simulations with Geant4-10.5 for two
 9 detector geometries, which are shown in Figure 2.



Figure 2. Tested scintillator geometries.

10 Because we planned to use small scintillator samples ~ 1 mm³, we decided to revise data
 11 on their emission spectra. The main reason is the fact that the excitation energy of the primary
 12 fluorophore is transferred to molecules of the spectrum shifter by the radiation transfer. For small

¹<https://www.caen.it>

²<http://www.ti.com>

1 scintillator samples of $\sim 150\mu\text{m}$, the probability of these UV photons escaping from the sensitive
 2 detector volume can no longer be considered negligible [7]. Unfortunately, the detection efficiency
 3 of plastic scintillators is significantly smaller in comparison with inorganic single crystals and thus
 4 it is rather hard to get reliable data under X-rays for small samples. Therefore, we just tested
 5 samples with dimensions of 9 x 9 x 5 mm and 9 x 9 x 1 mm. All the faces of the scintillators
 6 were mechanically polished. The top and side faces were coated with the EJ-510 paint. The
 7 measurements of the emission spectra of scintillator under X-rays were carried out on a stand
 8 based on the monochromator MDR-12U (LOMO, St.Petersburg), equipped with a photon-counting
 9 head H9319-01 (HAMAMATSU). The scintillators were irradiated by an X-ray tube at 100 kVp.
 10 Additionally, we compared the emission spectra when the scintillator was excited by an ultraviolet
 11 (UV) light-emitting diode (UVTOP300-HL-TO39, ROITHNER LASERTECHNIK GmbH)³ with
 12 a wavelength of 305 nm, near the maximum of photoabsorption of the primary fluorophore. In this
 13 case, the fluorescence spectra of the scintillator were measured by two methods: light transmission
 14 through a sample and light reflectance from a sample. Figure 3 demonstrates the emission spectra
 15 of the scintillator under different conditions.

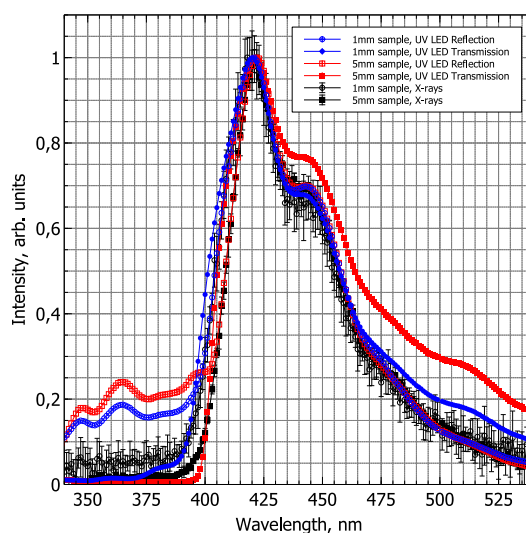


Figure 3. Light emission spectra of SC-301 scintillator under different conditions.

16 It is seen that under X-rays a thinner sample demonstrates a noticeable light output at a
 17 wavelength of less than 420 nm. The behavior of the emission spectra under UV excitation depends
 18 strongly on the layout. In the transmission method, we can observe significant self-absorption at
 19 lower wavelengths. In the reflection method, we can see significant contribution from the primary
 20 fluorophore of the scintillator with a maximum near 360 nm. In our later research, we used an
 21 X-ray excited emission spectrum for a 1 mm sample.

22 In the simulations, we compared two types of scintillator surfaces: the ground-back-painted
 23 to describe the diffuse light scattering of the white paint EJ-510 (Eljen Technology)⁴ and polished
 24 aluminum.

³<http://www.roithner-laser.com>

⁴<https://eljentechnology.com>

1 We used the following settings for the stepping process for all particles (e⁺, muons/hardons)
 2 in the scintillator: the maximum fraction of energy loss in a step of 0.1, a maximum step of 5 μm ,
 3 a 'Production Cut' parameter of 5 μm , and a Birks constant of 0.133 mm/MeV. This combination
 4 of parameters provided realistic results in comparison with experimental data that were obtained
 5 during evaluations of scintillator materials [8].

6 The POF was simulated as a PMMA core with a diameter of 980 μm , cladding 10 μm thick
 7 made of amorphous fluoropolymer CYTOP⁵, and outer coating made of black polyethylene. The
 8 length of POFs was 8.5 m. Spectral data on PMMA absorption length were reconstructed from
 9 technical data on PMMA-based ESKA polymer optical fiber (MITSUBISHI CHEMICAL). To
 10 extend the CYTOP refraction data to the visible wavelength range, the manufacturer data were
 11 approximated by the following equation:

$$n^2 - 1 = \frac{2.63483 \cdot \lambda^2}{3.09517 \cdot \lambda^2 - 0.0028} - \frac{0.17975 \cdot \lambda^2}{1.97329 \cdot \lambda^2 + 0.33579}, \quad (3.1)$$

12 where λ is expressed in μm . In the simulations, the optical contact between the scintillator and
 13 POF was filled with the most popular technical polymeric material, polydimethylsiloxane with a
 14 thickness of 10 μm . The main properties of the optical components with references are presented in
 15 Table 2.

Table 2. Main parameters of optical materials used in the simulations.

Parameter	Value	Source
EJ-510 Reflection	depending on wavelength	[9]
EJ-510 Refraction index	1.61	[10]
Polystyrene refraction index	depending on wavelength	[11]
Polystyrene absorption length	depending on wavelength	[12]
Polydimethylsiloxane refraction index	depending on wavelength	[13]
PMMA Refraction index	depending on wavelength	[14]
PMMA absorption length	depending on wavelength	[15]
CYTOP Refraction index	depending on wavelength	[16]
CYTOP absorption length	100 m	

16 As a photosensor, we planned to use a MPPC S13360-3050CS. Therefore its quantum efficiency
 17 was taken from manufacturer data [17] and was used to describe the sensitivity of a light detector
 18 installed at the distal end of the POF. The results of the simulation and the expected numbers of
 19 detected optical photons are shown in Table 3.

20 The low probability of light capture by the optical fiber leads to the fact that only ~ 5 percent of
 21 optical photons produced in the scintillator will be detected. The application of aluminum coating
 22 on the scintillator ensures no benefits over the white paint. Although a semi-ball shaped scintillator
 23 suggests a slightly higher signal value, in further experiments, we used cylindrical scintillators,
 24 which are easier in production.

⁵<http://www.agc-chemicals.com/jp/en/fluorine/products/detail/index.html?pCode=JP-EN-F019>

Table 3. Expected number of detected optical photons in different configurations. For comparison, when a neutron is captured by a boron atom in the scintillator, ~ 630 photons are produced.

Shape	Coating	Number of detected optical photons
Cylinder, POF length of 8.5 m	All sides: EJ-510	33.7
Cylinder	Side walls: EJ-510, Top: Al reflector	28.9
Cylinder	Side walls: Al reflector, Top: EJ-510	25.6
Cylinder	All sides: Al reflector	15.6
Semi-ball	EJ-510	35.3
Semi-ball	Al reflector	19.4

1 4 Initial trials.

2 To evaluate this detector approach we made several tests at the BINP BNCT facility. The cylindrical
 3 scintillators with a diameter of 1 mm and a length of 1 mm were cut from scintillator blocks. The
 4 output window of the scintillator was polished and the other sides were coated with the EJ-510
 5 paint. The scintillators were assembled with POFs with the length of 8.5 m and protected from
 6 ambient light by a light-tight housing. The optical coupling between a scintillator and POF was
 7 the optical grease BC-630 (Saint-Gobain Crystals)⁶. The detectors were installed at a distance of
 8 ~ 20 cm from the neutron producing target. Optical pulses were detected by MPPC S13360-3050CS
 9 (HAMAMATSU), followed by a home-made amplifier based on THS3202 (Texas Instruments), and
 10 processed by a digital acquisition system DT5790 (CAEN) in the charge-integration mode with a
 11 gate of 32 ns. During the tests, the temperature of the MPPC was stabilized at 0°C .

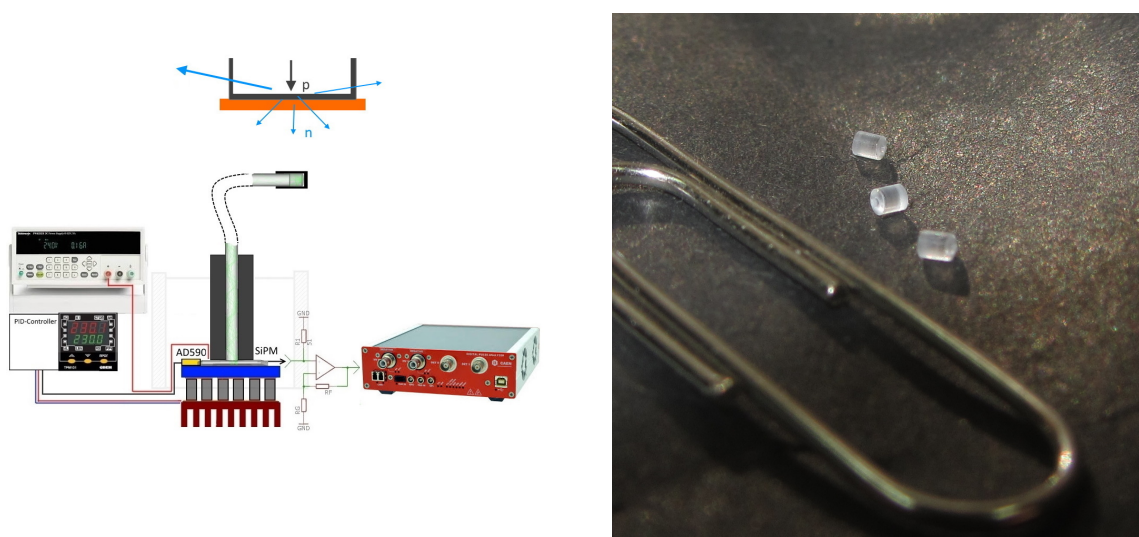


Figure 4. Experimental setup and produced scintillator samples just after mechanical processing.

12 Figure 4 demonstrates the experimental setup (left) and produced scintillator samples just after

⁶<https://www.crystals.saint-gobain.com/products/assembly-materials>

1 cutting (right).

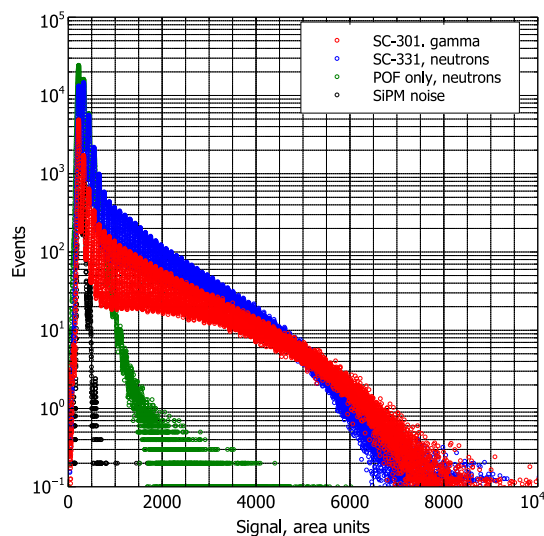


Figure 5. Measured charge spectra in different irradiation conditions.

2 Figure 5 shows examples of the measured spectra: the SiPM noise when the accelerator
 3 was off; signals from the SC-301 scintillators when the accelerator operated below the neutron
 4 production threshold; signals from the SC-331 (boron-enriched) scintillators when the accelerator
 5 operated in the neutron production mode; signals from a POF without scintillator under neutron
 6 irradiation, the surface that opposite to its exit window coated with the white paint. From the
 7 presented data we can see that in the region of signals below ~ 10 photo-electrons, the intrinsic
 8 SiPM noise and the Cherenkov light generated by the secondary high-energy electrons in the optical
 9 fiber give a dominant contribution. When the accelerator operates in the neutron production mode,
 10 the spectrum from the SC-331 scintillator demonstrates an excess of low amplitude events, but the
 11 detected neutrons do not form a clearly distinguished peak against the background.

12 **5 Dual threshold approach.**

13 The fact that boron-enriched and boron-less scintillators have slightly different light outputs leads
 14 to necessity of different detection thresholds in the readout electronics. A neutron-gamma counting
 15 detector was realized based on EASIROC ASIC [18]. The EASIROC channel integrates an 8-bit
 16 DAC, a variable gain preamplifier, and a fast shaper (15 ns), followed by a discriminator. In our
 17 design, two ASICs were connected in parallel to have the possibility of counting the same events
 18 with two different thresholds. Four MPPC S13360-3050CS and two pairs of scintillator-over-fiber
 19 detectors formed two neutron detection channels. In one pair we used the ASAHI SB-1000 optical
 20 fiber and in the second one MITSUBISHI CK-40. The data were continuously accumulated in a
 21 5 ms interval and sent to the computer for further processing. During the operation, the control
 22 software measured the environmental temperature and adjusted the bias voltage to keep the SiPM
 23 gain constant. Figure 6 demonstrates a simplified block diagram of the detector electronics (left)
 24 and the experimental setup (right).

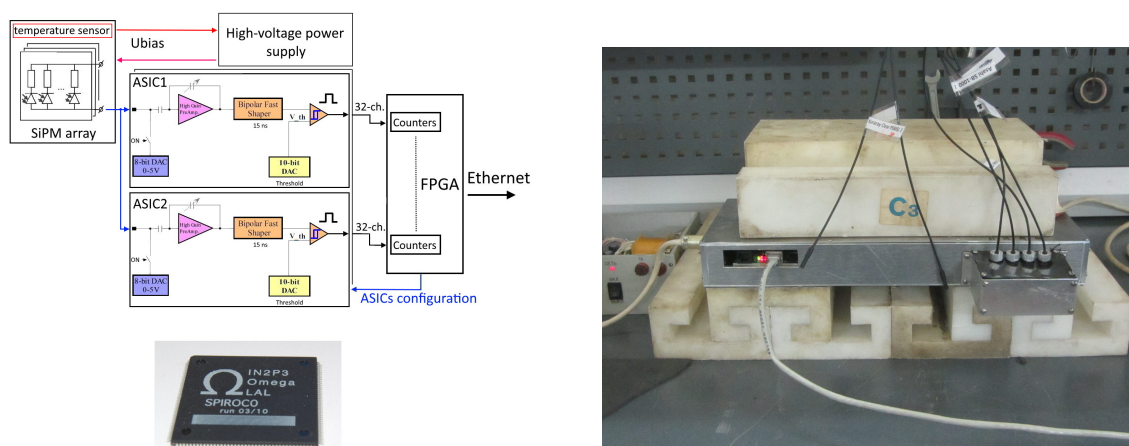


Figure 6. Simplified block diagram of multichannel system and experimental setup.

6 Results and discussion.

- Figure 7 demonstrates the average count rate per 5 ms as a function of the threshold when the accelerator operates in the neutron production mode.

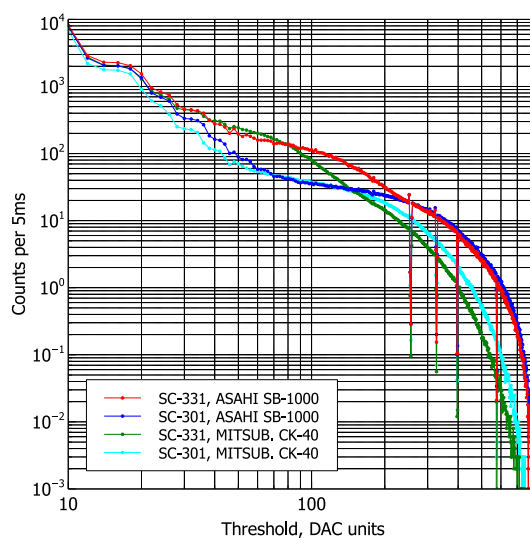


Figure 7. Mean signal value in detector channels per 5 ms vs. detection threshold under neutron irradiation.

- When the threshold value is less than ~ 200 DAC units, the contribution of the neutron component is visible in the data from registration channels using a scintillator with boron. For regular operation, we adjusted the detection threshold of ASICs near ~ 50 DAC units so that when both detectors (with and without boron) were irradiated with gamma radiation only, they recorded the same event rates. The true value of the neutron flux was restored as the difference between the counting rates in the ASIC1 channels registering the signal from the scintillator enriched with

1 boron and the counting rates in the corresponding ASIC2 channels recording the signal from the
 2 conventional scintillator.

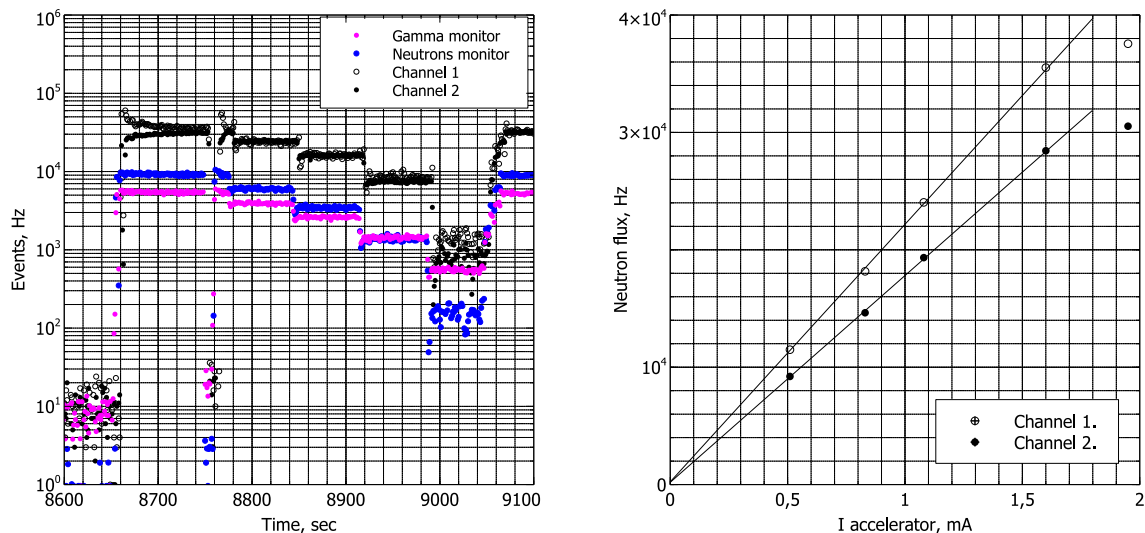


Figure 8. Sample of real-time measurements of neutron flux on BNCT facility (left) and detected neutron flux in detector channels as a function of accelerator current (right).

3 Figure 8(left) shows a sample of the real-time measurements of the thermal neutron flux when
 4 the accelerating voltage of the BNCT facility was gradually decreased below the neutron production
 5 threshold. For comparison, data from an independent gamma-neutron detection system based on
 6 a cerium-activated lithium-silicate glass scintillator with a photomultiplier readout are added [19].
 7 Figure 8(right) demonstrates the signal dependence on the accelerator current for a stationary proton
 8 beam with an energy of 2 MeV. The detector demonstrated a good linearity of up to ~ 1.7 mA,
 9 which was limited by the technical specifications of the accelerator at that time. It is planned that
 10 future modifications of the accelerator will operate at up to 10 mA and the detector linearity should
 11 be revised. From the last figure it is seen that the two detectors have different responses. The
 12 explanation is the fact that the detectors have slightly different sensitivities. Another reason is the
 13 difference in the magnitude of the neutron flux at the locations of the detectors, which can vary
 14 when the proton beam is positioned on the target. Another important pending issue is the efficiency
 15 of light collection on a photodetector. The magnitudes of signals observed in the experiment from
 16 neutrons captured in the scintillator were about 2 times less than expected from the simulation. The
 17 main reason can be in the production technology of such small scintillator samples. This time we
 18 mechanically cut the samples from rather big blocks and polished the output window to provide
 19 optical transparency only. In the future, this production stage should be revised to provide well
 20 reproducible results.

21 7 Conclusion.

22 In this study, we tested the scintillator-over-fiber approach to design a neutron sensitive detector
 23 for the BNCT. The presented results showed that the proposed system could be used successfully

1 for the monitoring of neutron flux. The application of SiPM instead of vacuum photomultipliers
 2 dramatically simplified the detector design and made it possible to realize a compact multichannel
 3 readout system. Anyway, there are several issues to address to ensure reliable operation of the
 4 detector. In particular, it is necessary to optimize the design of the detector to ensure maximum
 5 signal magnitude and to study the long-term stability of the detector components.

6 **8 Acknowledgments**

7 We would like to thank the BINP BNCT team for their help during the test sessions. The research
 8 is partially supported by a grant of the Russian Science Foundation (project №19-72-30005).

9 **References**

- 10 [1] D. Moro et al. *BNCT dosimetry performed with a mini twin tissue-equivalent proportional counters*
 11 *(TEPC)*. Applied Radiation and Isotopes. 67 (2009) pp.171-174
 12 <https://doi.org/10.1016/j.apradiso.2009.03.042>
- 13 [2] A.S. Beddar, T.R. Mackie, F.H. Attix, *Water-equivalent plastic scintillation detectors for high-energy*
 14 *beam dosimetry: I. Physical characteristics and theoretical considerations*. Phys. Med. Biol. Vol. 37
 15 (1992) pp.1883-1900 <https://doi.org/10.1088/0031-9155/37/10/006>
- 16 [3] M. Ishikawa et al. *Early clinical experience utilizing scintillator with optical fiber (SOF) detector in*
 17 *clinical boron neutron capture therapy: Its issues and solutions*. Radiation Oncology 11(1) (2016)
 18 105. <https://doi.org/10.1186/s13014-016-0680-0>
- 19 [4] M. Ishikawa et al. *Development of real-time thermal neutron monitor using boron-loaded plastic*
 20 *scintillator with optical fiber for boron neutron capture therapy*. Appl. Radiat. Isot. 61(5) (2004)
 21 775-779 <https://doi.org/10.1016/j.apradiso.2004.05.053>
- 22 [5] D. Kasatov et al. *The accelerator neutron source for boron neutron capture therapy*. Journal of
 23 Physics: Conference Series 769 (2016) 012064
 24 <https://doi.org/10.1088/1742-6596/769/1/012064>
- 25 [6] V. Rykalin et al. *Development of the Polystyrene Scintillator Technology and Particle Detectors on*
 26 *Their Base*. Journal of Physical Science and Application. Vol. 5, (2015) pp.6-13.
 27 <https://doi.org/10.17265/2159-5348/2015.01.002>
- 28 [7] R.N. Nurmukhametov et al. *Fluorescence and absorption of a polystyrene-based scintillator exposed*
 29 *to UV laser radiation*. Journal of Applied Spectroscopy Vol. 74, Issue 6, (2007) pp.824-830
 30 <https://doi.org/10.1007/s10812-007-0128-2>
- 31 [8] V.V. Porosev, G.A. Savinov. *Evaluation of boron-enriched plastic scintillator for thermal neutron*
 32 *detection*. 2019 JINST 14 P06003 <https://doi.org/10.1088/1748-0221/14/06/P06003>
- 33 [9] Eljen Technology. <https://eljentechnology.com/products/accessories/ej-510-ej-520>
- 34 [10] M. Janecek, W.W. Moses. *Simulating Scintillator Light Collection Using Measured Optical*
 35 *Reflectance*. IEEE Transactions on Nuclear Science. Vol. 57, no. 3, (2010) pp. 964-970
 36 <https://doi.org/10.1109/TNS.2010.2042731>
- 37 [11] <https://refractiveindex.info/?shelf=3d&book=plastics&page=ps>
- 38 [12] J. Argyriades et al. *Spectral modeling of scintillator for the NEMO-3 and SuperNEMO detectors*.
 39 Nucl. Instrum. Meth. A625 (2011) pp.20-28 <https://doi.org/10.1016/j.nima.2010.09.027>

- 1 [13] [https://refractiveindex.info/?shelf=organic&book=polydimethylsiloxane&page=](https://refractiveindex.info/?shelf=organic&book=polydimethylsiloxane&page=Schneider-Sylgard184)
2 [Schneider-Sylgard184](https://refractiveindex.info/?shelf=organic&book=polydimethylsiloxane&page=Schneider-Sylgard184)
- 3 [14] [https://refractiveindex.info/?shelf=organic&book=poly\(methyl_methacrylate\)](https://refractiveindex.info/?shelf=organic&book=poly(methyl_methacrylate)&page=Szczurowski)
4 [&page=Szczurowski](https://refractiveindex.info/?shelf=organic&book=poly(methyl_methacrylate)&page=Szczurowski)
- 5 [15] Mitsubishi Chemical Corporation.
6 https://www.pofeska.com/pofeskae/download/pdf/technical%20data_01.pdf
- 7 [16] Asahi Glass Company. [http://www.agc-chemicals.com/file.jsp?id=jp/en/fluorine/](http://www.agc-chemicals.com/file.jsp?id=jp/en/fluorine/products/cytop/download/pdf/CYTOP_EN_Brochure.pdf)
8 [products/cytop/download/pdf/CYTOP_EN_Brochure.pdf](http://www.agc-chemicals.com/file.jsp?id=jp/en/fluorine/products/cytop/download/pdf/CYTOP_EN_Brochure.pdf)
- 9 [17] https://www.hamamatsu.com/resources/pdf/ssd/s13360_series_kapd1052e.pdf
- 10 [18] S. Callier, C.D. Taille, G. Martin-Chassard, L. Raux, *EASIROC, an easy and versatile ReadOut device*
11 *for SiPM*. Physics Procedia 37 (2012) pp.1569-1576
12 <https://doi.org/10.1016/j.phpro.2012.02.486>
- 13 [19] V. Aleynik et. al. *New technical solution for using the time-of-flight technique to measure neutron*
14 *spectra*. Applied Radiation and Isotopes. Vol. 69 (2011) pp.1639-1641
15 <https://doi.org/10.1016/j.apradiso.2011.02.014>